Available online at www.sciencedirect.com
SCIENCE DIRECT®
Journal of Nuclear Materials 343 (2005) 313–317
journal of nuclear materials
www.elsevier.com/locate/jnucmat

Effect of ion irradiation and implantation of H and He on the corrosion behavior of austenitic stainless steel

Y. Nemoto *, Y. Miwa, Y. Kaji, T. Tsukada

Department of Nuclear Energy System, Japan Atomic Energy Research Institute, Shirakata-Shirane 2–4, Tokai-mura, Naka-gun, Ibaraki-ken 319-1195, Japan

Abstract

It is important to evaluate the effect of irradiation on the corrosion behavior of materials to be used in spallation neutron sources. Solution annealed high purity Fe–18Cr–12Ni specimens were used in this study. Ni^{3+} and H^{+} or He^{2+} ions were injected at 473–773 K. After corrosion test, the specimens were examined with atomic force microscope (AFM) to evaluate the corrosion behavior. It was shown that the corrosion rate of the irradiated area increased with increasing dose and temperature. H implantation accelerated corrosion. On the other hand, He implantation seemed to suppress corrosion. Mechanisms for these effects of the different irradiation conditions on the corrosion behavior are discussed.

PACS: 28.50.Ft; 61.80.−x; 41.75.Ak; 82.45.Bb; 68.37.Ps; 25.55.−e

1. Introduction

Liquid metals are expected to be used as neutron spallation targets, i.e. mercury for intensive neutron sources and lead–bismuth for accelerator-driven systems (ADSs) [1–3]. Candidate structural materials for the target are type316 austenitic stainless steel and F82H ferritic steel. In the case of the target assembly concept for the J. PARC project, target vessel will be cooled by heavy water or light water [4]. Therefore, corrosion resistance of these materials after irradiation needs to be addressed. Moreover, high energy protons and neutrons will irradiate the structural materials in or close to the proton beam [5]. It is known that radiation damage such as radiation-induced segregation, dislocation loops, precipitates, etc. may cause a degradation of the corrosion resistance of materials [6–16]. However, there were not enough studies about the corrosion behavior of the candidate structural materials after irradiation.

The aim of this work is to study the effects of different irradiation condition on the corrosion behavior on stainless steel. It was difficult to evaluate corrosion behavior on irradiated materials by conventional techniques such as electrochemical potential reactivation (EPR) method [14], therefore, the authors developed a new evaluation method using atomic force microscope (AFM) in previous studies [15–18]. The AFM method succeeded to obtain quantitative results relative to the corrosion behavior of ion irradiated materials. Therefore, it was applied to the study of the corrosion

* Corresponding author. Tel.: +81 29 282 5348; fax: +81 29 282 6122.
E-mail address: y.nemoto@popsvr.tokai.jaeri.go.jp (Y. Nemoto).

0022-3115/$ - see front matter
doi:10.1016/j.jnucmat.2005.01.024

behavior of materials after ion irradiations, which simulate the irradiation conditions of structural materials in a spallation neutron source. The operating temperature is expected to be about 473 K or below [5]. Radiation damage would amount to 35 dpa per year [4]. Moreover, considerable quantities of transmutation products, particularly hydrogen and helium, will be generated due to the exposure to a high flux of 1 GeV protons and associated neutrons at rate of 500–1000 appm H/dpa and 50–200 appm He/dpa [5,19]. Therefore, the effects of radiation damage, irradiation temperature, H and He on the corrosion behavior was studied in this work.

2. Experimental

Chemical composition of the stainless steel used in this study is listed in Table 1. The stainless steel was high purity Fe–18Cr–12Ni alloy that was solution annealed at 1323 K for 30 min. Specimens 6 mm in length, 3 mm in width and 0.3 mm in thickness was fabricated. The surface of the specimens was mechanically polished with emery papers and diamond paste of 0.3 μm diameter, then electrochemically polished in a solution with H_3PO_4 54%, H_2SO_4 36%, CH_3OH 10% at about 280 K with a potential of 18 V for 5 s.

Ion irradiation experiments of these specimens were conducted at Takasaki Ion Accelerators for Advanced Radiation Application (TIARA) of Japan Atomic Energy Research Institute (JAERI). Twelve mega-electron volt 12 MeV Ni^{3+} ions were injected in order to produce radiation damage, and H^+ or He^{2+} ions were synergistically implanted in the specimens. The defect production rate by Ni^{3+} ion irradiation was about 9.2×10^{-4} dpa/s. Irradiation conditions are listed in Table 2. Radiation damage and ion concentration in this list were estimated at the position of the gas atoms concentration. Irradiation for the specimens was conducted at the side of sheet. Depth profiles of radiation damage and contents of implanted atoms were calculated by TRIM85 code, and typical implant concentration and depth profiles are shown in Fig. 1. The depth profile was almost the same for every irradiation conditions. H^+ and He^{2+} ions were implanted at depth of about 1.5 μm which does not correspond to the peak-damage region. Near the peak-damage region, implanted Ni^{3+} ion may affect radiation damage [7]. Therefore, the peak-damage region was avoided for H^+ and He^{2+} ion implantation.

Table 2
Irradiation conditions

Radiation damage (dpa)	Irradiation temperature (K)	Ratio of H/dpa (appm/dpa)	Ratio of He/dpa (appm/dpa)
5	473	0	0
5	573	0	0
5	673	0	0
5	773	0	0
35	473	0	0
35	573	0	0
35	673	0	0
70	573	0	0
35	473	50	0
35	573	50	0
35	573	500	0
35	473	0	50
35	573	0	50
35	673	0	50
35	573	0	500
35	673	0	500

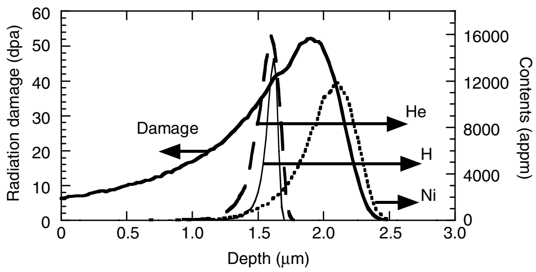

Fig. 1. Typical distributions of radiation damage and ion contents as function of the depth in specimens (35 dpa, 673 K, 500 H/dpa, 500 He/dpa). Major radiation damage was given by Ni^{3+} irradiation, and the damage given by gas atoms can be neglected.

To protect the irradiated surface during corrosion test, a copper film was plated on the irradiated specimens. The aqueous solution for Cu plating contains $CuSO_4$ 90 g, H_2SO_4 15 ml and pure water 475 ml. Plating was performed with a current density of about 0.03 A/cm^2, at ambient temperature with anode metal of pure Cu. After plating, side of specimens was mechanically polished as smooth as possible with alumina powder of 0.3 μm in diameter. Fig. 2 shows a sketch of the specimen after polishing. Corrosion test

Table 1
Chemical composition (wt%)

Cr	Ni	C	Si	Mn	P	S	Ti	N	Fe
18.17	12.27	0.003	0.01	1.36	0.001	0.0014	0.01	0.0014	Bal.

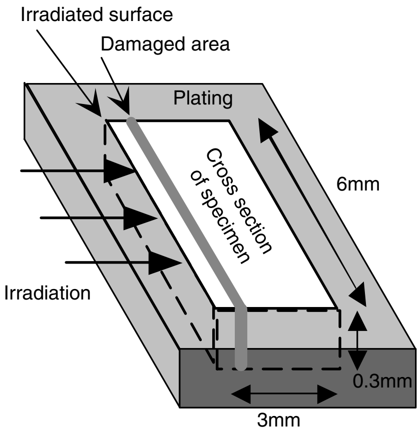

Fig. 2. Sketch of the specimen.

was conducted on the polished surface which is parallel to the irradiation direction.

Potentiostatic corrosion test followed by AFM measurement was applied in this work. A corrosion test at passivation potential (150 mV vs. Ag/AgCl) for 500 s in solution of 0.5 mol/l H_2SO_4 and 0.01 mol/l KCSN at 303 K gave acceptable surface condition for AFM evaluation [15,16].

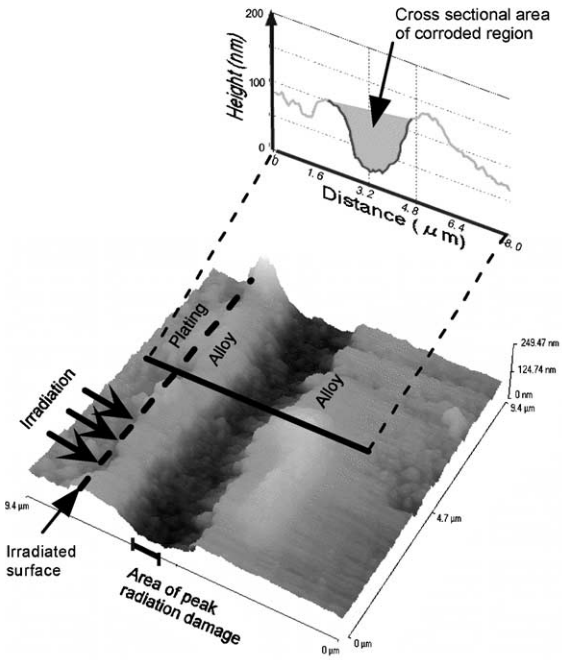

Fig. 3. Typical AFM topography on ion irradiated specimens [15,16]. This specimen was irradiated up to 35 dpa at 673 K, and corrosion test was conducted for 500 s.

3. Results

Typical AFM topography on the cross-sectional surface of an irradiated specimen after corrosion test is shown in Fig. 3 [15,16]. This specimen was irradiated at 673 K up to 35 dpa. Irradiated surface is indicated on left side of topography by dotted line, and the area of peak radiation damage was at depth of about 1.0–2.0 μm inside from the irradiated surface. The area of peak radiation damage was etched uniformly. The height distribution was measured along the line drawn on topography; that is the area of peak radiation damage. The corrosion rate was calculated from cross-sectional area of corroded region measured on height distribution graph as shown in Fig. 3 and corrosion testing time. Corrosion rate was used to compare corrosion behavior of the specimens irradiated with different irradiation condition.

Fig. 4 shows the dose dependence of the corrosion rate in the temperature range of 473–773 K. As radiation damage increased, depth of corroded region increased therefore, corrosion rate increased. And also the corrosion rate increased with irradiation temperature. Fig. 5 gives the effect of H/dpa ratio on the corrosion rate. Synergistic H implantation enhanced corrosion. In this case, depth of corroded region was increased with H content, and the corroded region seems to shift slightly closer to the irradiated surface. As seen in Fig. 6, on the other hand, synergistic He implantation

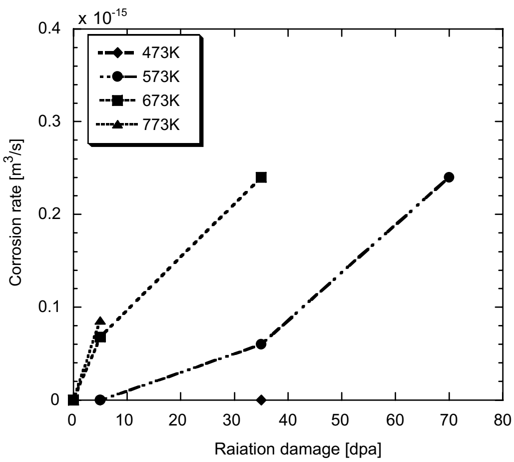

Fig. 4. Corrosion rate dependence on radiation damage.

seems to decrease the corrosion rate. In this case, the depth of corroded region decreased.

4. Discussion

In this study, the corrosion rate increased with increasing dose and irradiation temperature. Profile of Fig. 4 resembles dose and temperature dependence of

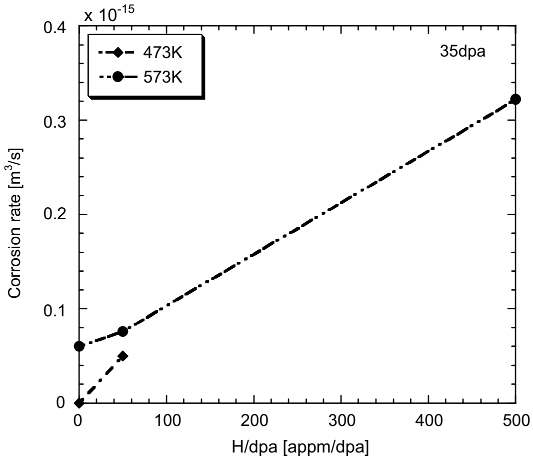

Fig. 5. Corrosion rate dependence on H content.

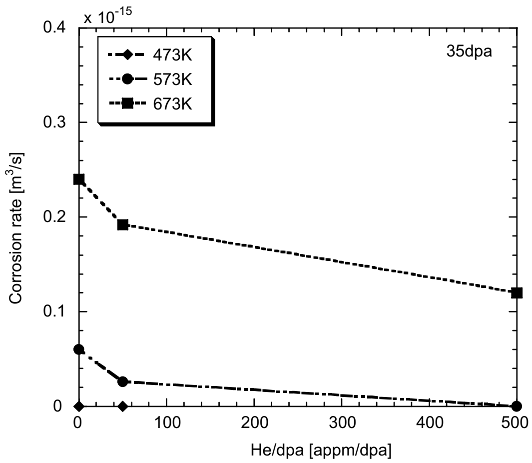

Fig. 6. Corrosion rate dependence on He content.

void swelling in former studies [20–26]. Therefore, the dependence of corrosion rate upon dose and temperature would be described with over saturation of vacancy. Vacancy diffuses to sink such as dislocation loops, precipitates, cavities and grain boundaries. At the same time, alloy element of Cr which is related to corrosion resistance is diffused away from the sink by exchange motion of lattice point and vacancy. It was reported in former studies that Cr depletion was observed not only on grain boundaries but also on defects in grain matrix of irradiated materials [13,21]. Therefore, it is considered that increase of vacancy diffusion with dose and temperature led increase of Cr depleted area, and caused corrosion enhancement.

As seen in Fig. 5, implantation of H accelerated corrosion. Ohnuki et al. [22] suggested that H and interstitial interaction can be neglected. However, Wakai et al. [23] reported that D^+ ion irradiations gave higher radiation-induced segregation on Ni based alloys than that in the case of electron irradiations. They discussed that interaction between D atom and vacancy might enhance radiation-induced segregation. D and H atoms would show similar behavior therefore, it is considered that synergistic H implantation with irradiation might cause higher Cr depletion at sinks. These could be considered as reasons of corrosion enhancement by H implantation in this work.

It was shown in this study that He implantation suppressed corrosion. To investigate the underlying mechanisms, detailed microscopic studies are required however, approvable explanation for the He effect can be proposed from the knowledge obtained in former studies [9,24–26]. He atoms are insoluble in stainless steels. They combine with vacancies preferentially, and form stable He-vacancy pairs. Therefore, the diffusion of vacancies to sinks and the loss of vacancies due to mutual recombination between vacancies and interstitials may be suppressed in materials containing He atoms. This mechanism could result in suppressing the growth of Cr depleted area at sinks. This is considered to be the main reason for the suppression of corrosion induced by He implantation.

5. Summary

In this study, experiments were conducted on ion irradiated Fe–18Cr–12Ni alloy, and the effect of irradiation condition on corrosion behavior was studied using AFM. Following results were obtained and the mechanisms were discussed:

(1) Increase of radiation damage increased corrosion rate.
(2) Increase of irradiation temperature increased corrosion rate.
(3) H implantation enhanced corrosion of irradiated specimens.
(4) He implantation suppressed corrosion of irradiated specimens.

Acknowledgement

The authors are grateful to Mr Tomio Suzuki, Drs Chiaki Kato, Hiroyasu Tanigawa and Eichi Wakai of Japan Atomic Energy Research Institute (JAERI) for many useful advises.

References

[1] K. Kikuchi, T. Sasa, S. Ishikura, K. Mukugi, T. Kai, N. Ouchi, I. Ioka, J. Nucl. Mater. 296 (2001) 34.

[2] M. Garcia-Mazario, M. Hernandez-Mayoral, A.M. Lancha, J. Nucl. Mater. 296 (2001) 192.
[3] M. Futakawa, Y. Kurata, I. Ioka, S. Saito, A. Naito, S. Hamada, Y. Kogawa, JAERI-Review 2002-035, Japan Atomic Energy Research Institute, 2002, p. 152.
[4] M. Kaminaga, R. Hino, K. Haga, T. Aso, H. Kinoshita, H. Kogawa, S. Sasaki, S. Ishikura, A. Terada, K. Kobayashi, J. Adachi, T. Teraoku, T. Takahashi, J. Akimoto, S. Honmura, in: Proceedings of Second Workshop on the Materials Technology for Spallation Neutron Source, KEK Proceedings 2001-11, High Energy Accelerator Research Organization, 2001, p. 91.
[5] E.H. Lee, J.D. Hunn, N. Hashimoto, L.K. Mansur, J. Nucl. Mater. 278 (2000) 266.
[6] M. Kodama, R. Katsura, J. Morisawa, S. Nishimura, S. Suzuki, K. Asano, K. Fukuya, K. Nakata, in: Proceedings of the Sixth International Symposium on Environmental Degradation of Materials in Nuclear Power Systems – Water Reactors, TMS, 1993, p. 583.
[7] T. Tsukada, JAERI-Research 98-007, Japan Atomic Energy Research Institute, 1998.
[8] P.L. Andresen, Stress Corrosion Cracking, ASM, New York, 1992, p. 181 (Chapter 6).
[9] S.M. Bruemmer, E.P. Simonen, P.M. Scott, P.L. Andresen, G.S. Was, J.L. Nelson, J. Nucl. Mater. 274 (1999) 299.
[10] J. Robertson, Corros. Sci. 32 (4) (1991) 443.
[11] P. Novak, R. Stefec, F. Fong, Corrosion 31 (10) (1975) 344.
[12] W.L. Clarke, R.L. Cowan, W.L. Walker, ASTM STP 656 (1978) 99.
[13] V.V. Sagaradze, S.S. Lapin, M.A. Kirk, J. Nucl. Mater. 280 (2000) 345.
[14] K. Kondou, A. Hasegawa, K. Abe, V. Kain, Y. Watanabe, in: Proceedings of the 10th International Conference on Environmental Degradation of Materials in Nuclear Power Systems – Water Reactors, NASE, 2001, CD-ROM.
[15] Y. Nemoto, Y. Miwa, H. Tsuji, T. Tsukada, in: Proceedings of the 11th International Conference on Nuclear Engineering, JSME, 2003, CD-ROM, ICONE11-36093.
[16] Y. Nemoto, Y. Miwa, Y. Kaji, H. Tsuji, T. Tsukada, in: Proceedings of the 11th International Symposium on Environmental Degradation of Materials in Nuclear Power Systems – Water Reactors, ANS, 2003, p. 1185, CD-ROM.
[17] L. Liu, T. Mitamura, M. Terasawa, Y. Takatani, S. Fukumoto, H. Tsubakino, J. Soc. Mat. Sci. Jpn. 49 (2) (2000) 222.
[18] M.P.H. Brongers, G.H. Koch, A.K. Agrawal, ASTM STP 1401 (2000) 394.
[19] E.H. Lee, J.D. Hunn, T.S. Byun, L.K. Mansur, J. Nucl. Mater. 280 (2000) 18.
[20] M. Terasawa, S. Nakahigashi, M. Koyama, J. Nucl. Sci. Technol. 20 (11) (1983) 929.
[21] E.A. Kenik, K. Hojou, J. Nucl. Mater. 191–194 (1992) 1331.
[22] S. Ohnuki, H. Takahashi, T. Takeyama, F. Wan, J. Nucl. Mater. 133&134 (1985) 459.
[23] E. Wakai, T. Ezawa, T. Tanabe, R. Oshima, Mater. Trans. 33 (10) (1992) 884.
[24] S. Hamada, Y.C. Zhang, Y. Miwa, D. Yamaki, Radiat. Phys. Chem. 50 (6) (1997) 555.
[25] T. Hashimoto, L.E. Rehn, P.R. Okamoto, Phys. Rev. B 38 (18) (1988) 868.
[26] K. Dewi, A. Hasegawa, S. Otsuka, K. Abe, Fusion Technol. 39 (2001) 585.